Supplementary Materials for

Declining Severe Fire Activity on Managed Lands in Equatorial Asia

Sean Sloan*, Bruno Locatelli, Niels Andela, Megan E. Cattau, David Gaveau, Luca Tacconi

*Corresponding author email: sean.sloan@viu.ca

This document includes:

Supplemental notes, figures, and tables by page number:

	Effect of Time as % of Effect of Precipitation with Respect to Rate of:			
	Severe Events	Very Severe Events	Severe Events	Very Severe Events
	Model Weighted by National Fire Activity		*Model Unweighted*	
Indonesia	58	39	67	49
Central-South Sumatra	85	19	113	69
Southern Kalimantan	40	34	51	43
Targeted Areas	43	18	65	45

Supplemental Table 1 The effect of the passage of time on rates of (a) Severe or (b) Very severe fire events per annum, as a percentage of the effects of total fire-season (July-December) precipitation, by region, 2002-2019.

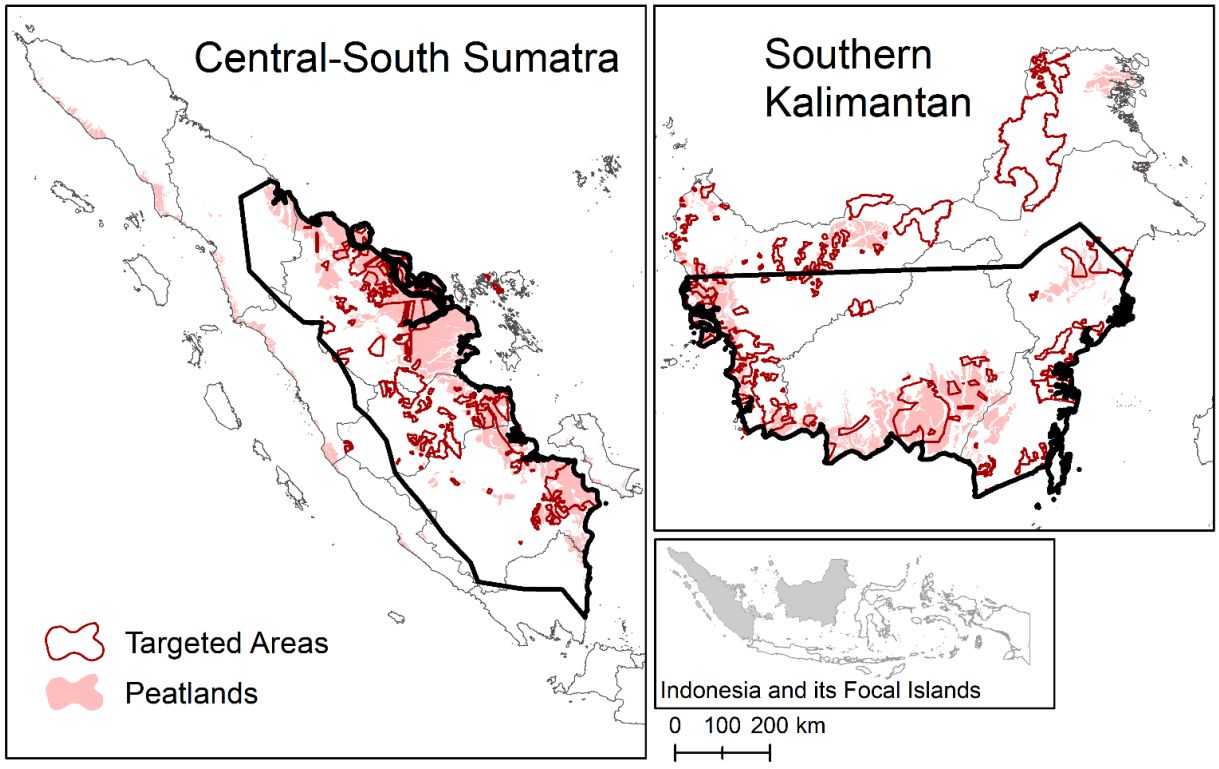

Supplemental Figure 1 Fire-affected regions of Central-South Sumatra and Southern Kalimantan relative to Peatland and areas targeted for fire prevention.

Notes: Thick black lines delineate the fire-affected regions.

Supplemental Note 1: The Severity of Seasonal Fire Activity

The severity of seasonal fire activity was given by the skewness (Eqn. 2) of fire-event severity scores (Eqn. 1) bi-annually. The precision, power, and bias of our skewness measure are similar to alternative measures designed for robustness to outliers[1-3], especially where frequency distributions are highly skewed and samples large, as is the case here. Below we detail various checks to the fidelity and robustness of our measure.

1.1 Sensitivity to the Specification of the Severity of Seasonal Fire Activity

Our measure of the severity of seasonal fire activity (Eqn. 2) discriminates amongst bi-annual seasons of extreme and moderate fire activity better than an alternative, direct measure of the total *magnitude* of fire severity. **Supplemental Figure 2a** illustrates this upon plotting our measures of severity of seasonal fire activity (Eqn. 2) against the seasonal magnitude of fire-activity severity, the latter expressed as the sum of cubed deviations of fire-event severity scores per bi-annual season relative to the mean severity score of 2002-2019:

$$\text{Total Cubed Deviations of Fire-Event Severity}_t \text{ from Grand Mean} = \sum\left(X_{it} - \bar{\bar{X}}\right)^3 \quad \text{(S1)}$$

where, for a given region, X_{it} is the severity of the i^{th} fire event for bi-annual season t; and $\bar{\bar{X}}$ is the mean fire-event severity of 2002-2019, termed the grand mean. Eqn. S1 is analogous to the cubed term in Eqn. 2 and similarly heavily 'weights' larger deviations via its cubic exponent. In principle, Eqn. S1 should aptly discriminate bi-annual seasons with respect to relative extremeness of their fire activity, consistent with common understanding of the relative severity of fire seasons historically, where extreme fire actively entails relatively large and frequent positive deviations from the grand mean.

Our original measure of seasonal severity (Eqn. 2) significantly correlates with the alternative measure (Eqn. S1) but also distinguishes between critical dimensions of extreme fire activity conflated by the alternative measure (Eqn. S1). **Supplemental Figure 2a** plots our original and alternative measures for Indonesia for all bi-annual seasons of 2002-2019 and reveals two dimensions defined by these measures. Dimension A describes heightened burning during fire seasons that coincided with relatively limited precipitation and generally also with elevated (≥0.5˚C) Oceanic Niño Index (ONI) values [4] over multiple months (e.g., late 2015, late 2018), with such months frequently comprising portions of broader El Niño periods (i.e., ONI ≥0.5˚C for >4 consecutive months), when burning is historically most extensive and severe. Virtually all fire activity during periods of heightened burning characterising Dimension A concentrated between mid-July and late October[5]. In contrast, Dimension B describes appreciable but relatively limited and less severe burning, occurring outside of fire seasons, largely during January and February prior to the onset of the first rainy period of the year (Sumatra), and coinciding either with the end of El Niño periods carried over from a prior year (e.g., early 2003, early 2005) or with other periods that were not particularly dry but which experienced relatively

Supplemental Figure 2 Relationship between severity of seasonal fire activity (Eqn. 2) and the seasonal magnitude of fire severity (Eqn. S1), by region and seasonal period.

Notes: Axis scales are not consistent between panels. Dimensions A and B in (*a*) were determined heuristically.

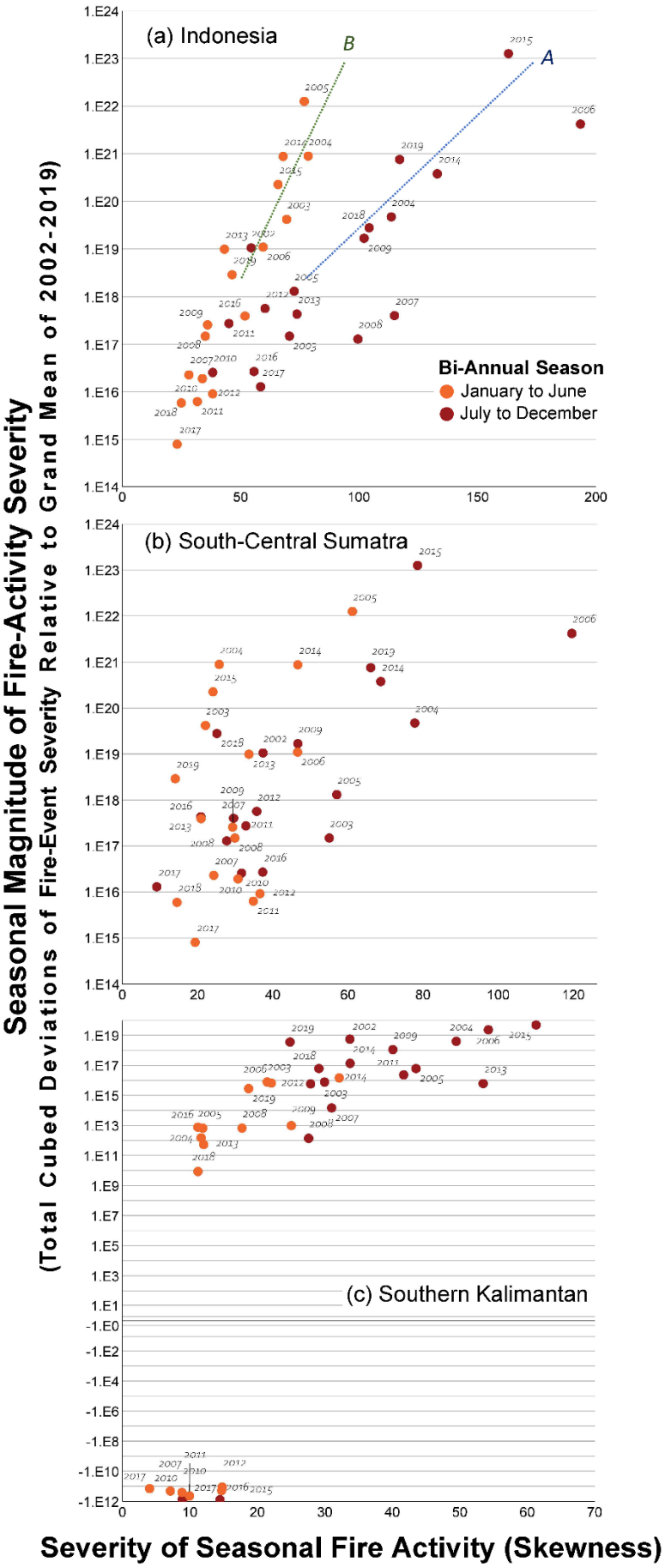

variable fire-event severity scores suggestive of elevated fire activity (e.g., early 2014). Dimensions A and B are also apparent for the two fire-affected regions (**Supplemental Figure 2b, Supplemental Figure 2c**). The fact that our measure of the severity of seasonal fire activity correlates with the alternative measure pertaining to absolute severity magnitude while also discriminating between dimensions A and B qualifies it as the superior indicator of fire-activity extreme and extent.

We further scrutinised the severity of seasonal fire activity with respect to the robustness of modelled temporal trends thereof (**Figure 3**). As per Eqn. 2, our measure of seasonal severity reflects deviations of fire-event severity scores relative to the seasonal (bi-annual) mean severity. Given variability amongst seasonal means, with potential implications for the modelled trends in seasonal severity, we re-fit our models of **Figure 3** while holding means constant. Specifically, for each region of interest, we substituted the seasonal mean severity $\bar{X}_t$ in Eqn. 2 with the grand mean fire-event severity score for 2002-2019, $\bar{\bar{X}}$, defined above. Subsequently, for the resultant, alternative metric of seasonal severity, we re-fit

regressions on seasonal precipitation and time elapsed since 2002. The results of these alternative regressions are largely consistent with the regressions underlying **Figure 3**. Controlling for precipitation, the alternative metric of seasonal severity declined significantly with time in South-Central Sumatra ($p<0.05$); declined moderately in the Targeted Areas ($p=0.1$); and declined insignificantly in Southern Kalimantan and nationally. Alternative models' explanatory power was lower (R^2=0.34-0.50) than for the original models (**Supplemental Table 2**), seemingly due to weaker linear relationships between precipitation and the alternative metric of seasonal severity. Still, in South-Central Sumatra, the effect of time on the alternative metric was equivalent to that of the original model (**Supplemental Table 2**) in terms of contributions to model R^2. Methodological details for the alternative models are summarised below.

Methodological Details: Upon substituting grand mean $\bar{\bar{X}}$ for $\bar{X}_t$ in Eqn. 2 for a given region as above, the corresponding alternative metric of the severity of seasonal fire activity M was transformed as $\text{Sign}(M) \times (\text{Log}_{10}(1+|M|)$ prior to re-fitting the regression models. $Sign(M)$ equals -1 or +1 where M is negative or positive, respectively. This transformation approximates a standard logarithmic transformation but is also suitable for negative values (**Supplemental Figure 2c**). Transformation improved linear fit with seasonal total precipitation and, not incidentally, with the logarithm of seasonal severity (Eqn. 2). Seasonal periods of 2017 were excluded as extreme outliers for all regions but Indonesia.

1.2 Sensitivity of the Severity of Seasonal Fire Activity

Skewness measures such as Eqn. 2 are potentially subject to perverse variation unrelated to extreme fire-event impacts. Specifically, at least where skewness is moderate, skewness may decrease appreciably while holding constant the values and frequencies of the higher fire-event impact scores (Eqn. 1), should the relative frequencies of fire events with lower and intermediate impact scores decrease and increase, respectively. As detailed below, we examined the possibility in our data and find it irrelevant, given the acute skewness observed. Observed declines in seasonal severity described by skewness (**Figure 3**) are therefore considered largely a function of declines in the value and frequency of higher fire-event severity scores.

We tested the sensitivity of observed skewness over four scenarios that progressively replaced lower-value, higher-frequency fire-event severity scores with higher-value, lower-frequency scores. These scenarios progressively increased the central tendency of a given seasonal (bi-annual) frequency distribution of severity scores while holding constant those scores above the 75th percentile as well as the total number of fire events. The four scenarios are as follows:

- Scenario 1 – Fire-event severity scores of the 45-50th percentile replaced those of the 1-5th percentile;
- Scenario 2 – Fire-event severity scores of the 40-50th percentile replaced those of the 1-10th percentile;
- Scenario 3 – Fire-event severity scores of the 25-50th percentile replaced those of the 1-25th percentile;
- Scenario 4 – Fire-event severity scores of the 50-75th percentile replaced those of the 1-25th percentile.

Percentiles here are with respect to the fire events of a given seasonal period. Two such periods were examined – July-December of 2015 and January-June of 2017 – having respectively the maximum (61.3) and minimum (4.1) skewness for Southern Kalimantan over 2002-2019. Southern Kalimantan was selected for scrutiny because its skewness values are moderate compared to Central-South Sumatra and Indonesia (**Supplemental Figure 2**).

In the case of July-December 2015, all four scenarios were within 0.01% of the observed skewness. In the case of January-June 2017, scenarios 1, 2, 3 and 4 deviated from the observed skewness by less than 1%, 2%, 3%, and 1%, respectively. Hence, the possibility of perverse variation to observed skewness is dismissed.

*****

Region	Seasonal Severity Explained [R^2]$^{\phi}$(%)	Model Coefficient (Bias)†		Effect of Time Relative to Precipitation (%)$^{\|\|}$	Seasonal Severity Explained [R^2] by Time, Net of Precipitation¶ (%)	Durbin-Watson$^{\#}$ (Bias)†
		Precipitation [total mm]	*Time [No. Intervals]*			
Indonesia	54****	-9.154 E-6**** (2.34 e-7)	-0.34 (-0.01)	12	1	2.25 (-0.83)
Southern Kalimantan	53****	-1.36 e-5**** (-1.960 e-7)	-0.33*‡ (-0.01)	32	5	2.16 (-0.75)
Central-South Sumatra	45****	-3.448 e-5**** (5.094 e-7)	-0.84**§ (0.00)	62	16	1.92 (-0.60)
Targeted Areas	53****	-5.488 e-5** (3.288 e-7)	-0.30*‡ (-0.01)	30	4	1.60 (-0.40)

Supplemental Table 2 Regressions of the severity of seasonal fire activity on precipitation and time elapsed over 2002-2019, seasonally by region.

Significance: * p<0.1, ** p<0.05, *** p<0.01, **** p<0.001

Notes: (ϕ) R^2 according to final model of severity of seasonal fire activity (Eqn. 2) as a function of precipitation and the number of bi-annual seasonal intervals elapsed since July 2002, i.e., time. (†) Bias is the difference in the coefficient computed from the bootstrapped samples and the original sample, defined as the former less the latter; (‡) Variable is equally significant (p<0.1) in an equivalent model without bootstrapping; (§) Variable is more significant (p<0.001) in an equivalent model without bootstrapping; (||) Defined as the standardised coefficient for time expressed as a percentage of the standardised coefficient for precipitation; (¶) Increase to model R^2 upon including the time variable in the final model, after including the precipitation variable in a partial model. Both the final and partial models included constants; (#) Durbin-Watson tests reject the assumption of positive autocorrelation of residuals (Targeted Areas, Central-South Sumatra) or are conservatively inconclusive (Indonesia, Southern Kalimantan) at $p<0.05$[6], where Durbin-Watson test statistics are defined by observed values and their corresponding bias.

Supplemental Note 2: Land-Use/Cover Shifts and Extreme Fire Activity

2.1 Severe Fire Events for Land-Use/Cover Trend Analysis

For the analysis of land-use/cover relative frequency amongst fire events and ignitions (**Table 2**), we defined severe fire events as those comprised by either the top 25% of all AFDs (set (*a*) in *Methods*) or the top 25% of ignition AFDs (set (*b*)) in terms of the fire-event severity scores (Eqn. 1) of corresponding fire events of 2002-2019. Land-use/cover trends for sets (*a*) and (*b*) are given respectively in **Tables 2a** and **2b**. The minimum 'threshold' fire-event severity necessarily differed between severe fire events of set (*a*) (7268.8) and of set (*b*) (138.1). Both of these thresholds also differed from the 75th percentile severity threshold defining annual rates of severe fire events (**Figure 1**). Threshold differences between set (*a*) and set (*b*) owe to the fact that ignition AFDs are less concentrated amongst fire events with higher severity scores than are AFDs generally. The potential use of the threshold of set (*a*) to define set (*b*) would have selected too few ignition AFDs for reliable analysis in **Table 2b**. Conversely, defining severe fire events for **Table 2a** using the threshold of set (*b*) or that used to model rates of severe fire events would have proven too unselective by qualifying half or two-thirds of all AFDs of 2002-2019 as severe, respectively.

2.2 Model Sensitivity to the Effects of Recent Years of Severe Fire Activity

Both 2015 and 2019 are years of anomalously severe and extensive fire activity late in our 2002-2019 time series[5,7,8] (**Figure 1**). Accordingly, observations for these years may be relatively influential to the significance of trends in the prevalence of land uses/covers amongst fire events and ignitions, summarised in **Table 2**. Here, we experimentally exclude 2015 and 2019 from the models underlying **Table 2** to assess the effects of recent, anomalous fire activity on trends modelled for the full time series. Significant trends across the full time series in **Table 2** are generally robust to the exclusion of 2015 (**Supplemental Table 3)** or 2019 (**Supplemental Table 4**). Exclusions of 2015 and 2019 also highlight the centrality of such years of heightened burning to the ascendency of *flooded vegetation* amongst fire activity over 2002-2019 (**Table 2**). The following describes methodological details and observations.

2.2.1 Methodological Background

Table 2 summarises regression models describing changes to the relative frequency of land uses/covers amongst fire-activity sets *a-d (*see *Methods* in the main text). As elsewhere, these models were bootstrapped 1000 times to ensure reliable, robust significance estimates. Bootstrapping entailed randomly re-sampling the 2002-2019 time series with replacement to yield 1000 time series for as many models, ultimately summarised in **Table 2**. While all 1000 bootstrapped samples pertained to the full time series 2002-2019 and so had n=18 annual observations, most samples were 'partial' insofar as they randomly omitted one or more years and therefore randomly included other year(s) more than once. Along such lines, the models summarised in **Supplemental Table 3** and **Supplemental Table 4** are identical in design to those of **Table 2** but explicitly excluded observations for 2015 or 2019 from all 1000 bootstrapped samples, respectively.

Region	Land Use/Cover 2002-2019 Excluding 2015													
	Cleared/ Cultivated	*Mosaic Cropland*	*Mosaic Veg.*	*Forest*	*Mosaic Shrubland*	*Low/Sparse Vegetation*	*Flooded Vegetation*	*Cleared/ Cultivated*	*Mosaic Cropland*	*Mosaic Veg.*	*Forest*	*Mosaic Shrubland*	*Low/Sparse Vegetation*	*Flooded Vegetation*
	(a) Active-Fire Detections of Severe Fire Events							***(b) Ignition Active-Fire Detections of Severe Fire Events***						
Indonesia	0.07	-0.35	-0.03	**-0.86**	0.08	0.29	**0.55**	0.09	**-0.6**	-0.17	-0.05	0.15	**0.24**	**0.31**
Southern Kalimantan	0.19	-0.13	-0.2	**-0.78**	0.01	0.34	0.59	0	**-0.56**	-0.07	0.19	0.01	**0.26**	**0.16**
Central-South Sumatra	-0.34	0.06	0.35	**-0.66**	**0.01**	0.01	0.58	0.1	**-0.51**	-0.36	-0.09	0	**0.24**	**0.61**
Elsewhere	**0.74**	**-1.38**	**-0.48**	-0.59	0.13	0.32	**0.59**	0.21	**-0.74**	-0.13	-0.15	0.34	**0.22**	**0.19**
Peatland	0.16	0.18	0.1	**-1.15**	0	0.11	**0.62**	0.12	-0.15	-0.07	**-0.8**	0	0.22	**0.53**
Mineral Soil	0.05	**-1.9**	**-0.54**	0.32	0.22	**0.75**	**0.35**	0	**-0.93**	-0.18	**0.46**	0.25	**0.23**	**0.12**
Targeted Areas	0.23	0.19	-0.02	**-1.02**	-0.01	0.08	**0.56**	0.05	**-0.37**	0	-0.34	0	0.23	**0.45**
	(c) Active-Fire Detections of All Fire Events							***(d) Ignition Active-Fire Detections of All Fire Events***						
Indonesia	-0.05	**-0.49**	0.02	-0.18	0.05	**0.18**	**0.38**	**-0.1**	**-0.62**	0.06	0.12	0.06	**0.14**	**0.25**
Southern Kalimantan	-0.04	**-0.46**	0.04	-0.05	**0.01**	**0.26**	**0.22**	**-0.16**	**-0.62**	0.14	**0.3**	0.01	**0.18**	**0.11**
Central-South Sumatra	-0.28	-0.48	-0.08	-0.08	0	**0.14**	**0.75**	-0.13	**-0.77**	-0.19	**0.22**	0	**0.15**	**0.68**
Elsewhere	**0.17**	**-0.62**	0.02	-0.23	0.12	**0.16**	**0.18**	0.02	**-0.45**	0.16	-0.17	0.1	**0.11**	**0.08**
Peatland	-0.01	-0.09	0.12	**-0.9**	0	**0.17**	**0.72**	-0.19	-0.4	0.06	**-0.57**	0	**0.21**	**0.87**
Mineral Soil	-0.06	**-0.85**	0	**-0.37**	0.11	**0.17**	**0.1**	-0.11	**-0.72**	0.11	**0.34**	0.09	**0.12**	**0.06**
Targeted Areas	-0.02	-0.18	0.08	**-0.67**	0	0.16	**0.61**	**-0.18**	**-0.57**	0.1	-0.15	0	**0.22**	**0.58**

Supplemental Table 3 Percentage change in land uses/cover frequency across fire events per annum, for 2002-2019 omitting 2015, by region, for either (a) Active-fire detections of severe fire events, (b) Ignition active-fire detections of severe fire events, (c) Active-fire detections of all fire events, and (d) Ignition active-fire detections of all fire events.

Notes: Positive and negative values are interpreted as for **Table 2**. Blue and red cell borders respectively denote decreasing and increasing fire activity over 2002-2019 omitting 2015 and having of least moderate significance without Bonferroni correction (Thick border, $p<0.001$; Medium border, $p<0.01$; Dashed border, $p<0.05$). Cells with borders are also distinguished by bold text. Blue and orange cell shading respectively denote decreasing and increasing trends over the full time series 2002-2019 as per **Table 2** and having at least moderate significance without Bonferroni correction (dark shading, $p<0.001$; medium shading, $p<0.01$; light shading, $p<0.05$). Interpretation based on shading/borders denoting $p<0.01$ and $p<0.001$ is favoured according to Bonferroni adjustments. For all regions, including Indonesia, Java and the Lesser Sunda Islands are excluded.

In **Supplemental Table 3** and **Supplemental Table 4**, cells are formatted to indicate agreement between models of the full time series (**Table 2**) and the models excluding 2015 or 2019, respectively. Here, agreement is with respect to statistical significance. Cells' *shading* denote significance according to the full time series 2002-2019 and is therefore exactly as in **Table 2**. Cells' *border colour and thickness* denote significance according to models excluding 2015 or 2019. Thus, agreement between a cell's border and its shading indicates agreement between models for the full and partial time series.

As in **Table 2**, **Supplemental Table 3** and **Supplemental Table 4** report significance values without Boneronni adjustment. Bonferroni adjustments prioritise significance at $p<0.01$. Such an adjustment is proportional to the number land use/cover classes in our models (**Table 1**), not the product of classes, fire-activity sets, and/or regions, considering the nested nature of our regions and sets and that our main hypothesis concerns differences amongst classes, not regions or sets[9].

2.2.2 Model Sensitivity

Significant trends across the full time series (**Table 2)** are generally robust to the exclusion of 2015 (**Supplemental Table 3**) or 2019 (**Supplemental Table 4**). Significant decreases in the prevalence of *mosaic cropland* and *forest* are affirmed across all sets of fire activity for both partial time series (**Supplemental Table 3** and **Supplemental Table 4**, panels *a-d*). A partial exception to this consistency is that the models for either partial time series attribute weaker significance to the increasing prevalence of *flooded vegetation* amongst severe fire events. If excluding 2015, the significance of the increasing prevalence of *flooded vegetation* amongst severe fire events weakens but remains moderate, except for the two fire-affected regions, where it become non-significant (**Supplemental Table 3a**). If excluding 2019, trends in the prevalence of *flooded vegetation* amongst severe fire events become non-significant for all regions (**Supplemental Table 4a**). The trend for *flooded vegetation* remains significant for all other sets of fire activity, however, regardless of whether 2015 or 2019 is excluded (panels *b-d* **in Supplemental Table 3** and **Supplemental Table 4**).

Region	Land Use/Cover 2002-2018													
	Cleared/ Cultivated	*Mosaic Cropland*	*Mosaic Veg.*	*Forest*	*Mosaic Shrubland*	*Low/Sparse Vegetation*	*Flooded Vegetation*	*Cleared/ Cultivated*	*Mosaic Cropland*	*Mosaic Veg.*	*Forest*	*Mosaic Shrubland*	*Low/Sparse Vegetation*	*Flooded Vegetation*
	(a) Active-Fire Detections of Severe Fire Events							***(b) Ignition Active-Fire Detections of Severe Fire Events***						
Indonesia	0.07	**-1.0**	-0.31	**-0.90**	0.24	0.53	0.43	-0.04	**-0.75**	-0.19	0.19	0.19	**0.20**	**0.38**
Southern Kalimantan	0.48	**-0.50**	-0.31	**-0.73**	0.01	0.09	0.68	-0.09	**-0.68**	-0.10	0.35	0.00	0.20	**0.33**
Central-South Sumatra	0.03	-0.13	0.43	**-0.83**	0.00	-0.05	0.54	-0.06	**-0.67**	-0.21	0.07	0.00	**0.22**	**0.64**
Elsewhere	0.38	**-1.67**	**-0.47**	-0.66	0.57	0.45	0.45	0.16	**-0.80**	**-0.33**	0.11	0.44	**0.20**	**0.18**
Peatland	0.43	-0.08	0.37	**-1.30**	0.00	-0.05	0.64	0.00	-0.27	0.05	**-0.73**	0.00	0.19	**0.77**
Mineral Soil	-0.17	**-2.37**	**-0.73**	0.17	0.57	**0.96**	0.18	-0.12	**-1.05**	-0.20	**0.72**	0.31	**0.19**	**0.13**
Targeted Areas	0.62	0.15	-0.18	**-0.96**	-0.01	-0.23	0.62	-0.01	**-0.50**	0.02	-0.26	-0.01	0.13	**0.63**
	(c) Active-Fire Detections of All Fire Events							***(d) Ignition Active-Fire Detections of All Fire Events***						
Indonesia	-0.11	**-0.81**	0.00	0.03	**0.15**	**0.16**	**0.40**	-0.16	**-0.55**	-0.05	-0.05	0.14	0.10	**0.51**
Southern Kalimantan	0.00	**-0.70**	0.18	0.06	0.00	**0.16**	0.23	-0.21	**-0.49**	0.00	-0.02	-0.03	0.11	**0.64**
Central-South Sumatra	-0.19	**-0.85**	-0.25	0.06	0.00	0.15	**1.02**	-0.19	-0.39	0.01	-0.05	0.00	0.04	**0.56**
Elsewhere	0.05	**-0.72**	-0.04	-0.13	**0.26**	**0.18**	**0.14**	0.04	**-1.03**	**-0.29**	0.32	0.52	**0.20**	**0.19**
Peatland	0.01	-0.53	-0.04	**-0.78**	0.00	0.14	**1.21**	0.01	-0.06	0.04	**-0.83**	-0.04	0.02	**0.86**
Mineral Soil	**-0.15**	**-1.02**	-0.04	**0.48**	**0.22**	**0.19**	**0.09**	**-0.27**	**-1.16**	-0.15	**0.82**	0.33	**0.20**	**0.16**
Targeted Areas	0.10	-0.48	0.03	**-0.47**	0.00	0.02	**0.82**	0.15	-0.04	-0.01	**-0.69**	-0.12	-0.14	**0.84**

Supplemental Table 4 Percentage change in land uses/cover frequency across fire events per annum, for 2002-2018, by region, for either (a) Active-fire detections of severe fire events, (b) Ignition active-fire detections of severe fire events, (c) Active-fire detections of all fire events and (d) Ignition active-fire detections of all fire events.

Notes: Positive and negative values are interpreted as for **Table 2**. Blue and red cell borders respectively denote decreasing and increasing fire activity over 2002-2018 having of least moderate significance without Bonferroni correction (Thick border, $p<0.001$; Medium border, $p<0.01$; Dashed border, $p<0.05$). Cells with borders are also distinguished by bold text. Blue and orange cell shading respectively denote decreasing and increasing trends over the full time series 2002-2019 as per **Table 2** and having at least moderate significance without Bonferroni correction (dark shading, $p<0.001$; medium shading, $p<0.01$; light shading, $p<0.05$). Interpretation based on shading/borders denoting $p<0.01$ and $p<0.001$ is favoured according to Bonferroni adjustments. For all regions, including Indonesia, Java and the Lesser Sunda Islands are excluded.

The varying significance of the increasing prevalence of *flooded vegetation* between the full and partial time series underscores the key role played by years of heightened fire activity, such as years host to El Niño events, which were weighted relatively heavily in the models. In this respect, the varying significance is consistent with the concentration of severe fire activity on peatlands since the late 1990s[7] as well as the strong association between extensive peatland burning with drought. The weaker significance of the increasing prevalence of *flooded vegetation* amongst severe fire events for the partial time series may also reflect the following factors: (*i*) The relatively high inter-annual variability of land-use/cover frequencies amongst severe fire events, compared to other sets of fire activity (**Supplemental Figure 3**); and (*ii*) Differences in the geographies (**Figure 2a, 2b**) and land-use/cover compositions (**Supplemental Figure 3**) of severe fire events, compared to other sets of fire activity.

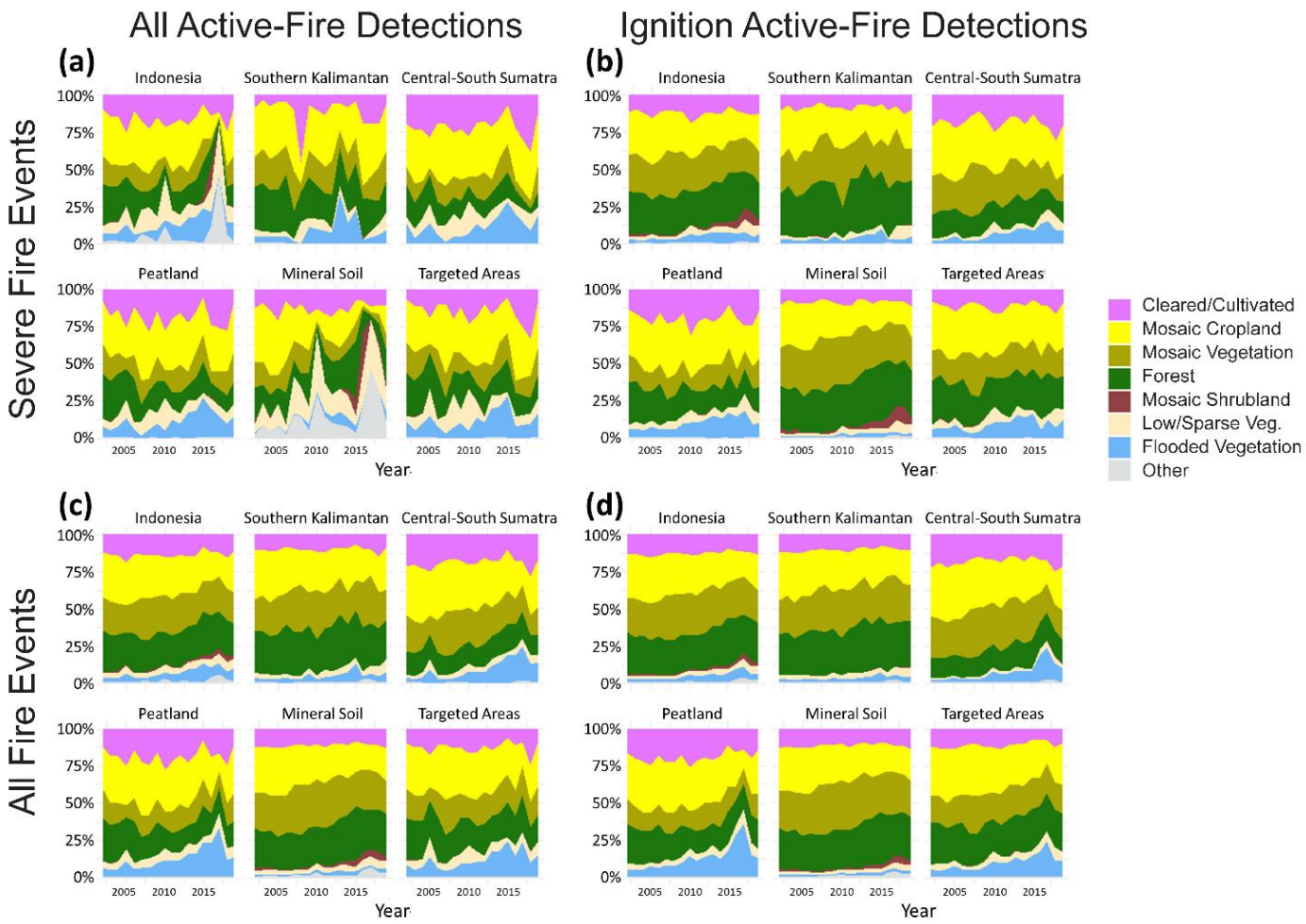

Supplemental Figure 3 Changing prevalence of land uses/covers across fire events, 2002-2019 as percentages of (a) Active-fire detections of severe fire events, (b) Ignition active-fire detections of severe fire events, (c) Active-fire detections of all fire events, and (d) Ignition active-fire detections of all fire events, by region.

*****

Supplemental Note 3: Land-Use/Cover Management Intensity

To verify and demonstrate the management intensities of our three land-use classes (*cleared/cultivated, mosaic cropland with >50% vegetation, and mosaic vegetation with <50% cropland*), we compared our land-use/cover classification (**Table 1**) against active land use visually interpreted using high-resolution satellite imagery. The notion of active land use pertains to relatively intensively-managed lands with clear signs of current usage (as of the observation year). Such lands are distinguished from those subject to low-intensity or sporadic use and/or degradation associated with proximate land use, typically being less managed or peripheral lands. Comparisons between our land-use/cover classification (**Table 1**) and visual interpretations of active land use were realised for 2015 across 7.5 Mha of Targeted Areas within the fire-affected regions of South-Central Sumatra and Southern Kalimantan (**Supplemental Figure 5**).

Active land use is defined as the predominance tilled lands, crops/planted trees (including saplings), and fresh clearings as visually apparent at 1:3000 to 1:12,000 scale in high-resolution imagery of Google Earth for 2015 ± two years. The interpreted high-resolution images were acquired for a variety of months and seasons, as determined by image availability per locale within Google Earth. Acquisition dates presumedly correspond largely to the relatively cloud-free months of June-November (Southern Kalimantan) and January-March and May-October (South-Central Sumatra). Mixed areas not under active use but still managed, exploited, or subject to human activity were largely excluded from the extent of active land use, although such areas were inevitably incorporated to a limited degree in the process of manual delineation. Such mixed areas include open but unplanted/untilled lands, older fallows/regrowth, sparse peripheral swidden cultivation, scrublands, and degraded forest, amongst others. When manually delineating active land-use polygons, no more than half of a given polygon hosted such mixed land covers. This proportion was generally far less in practice, however, e.g., ~1-20% per visual estimations. Further details on active land-use mapping are given by Sloan *et al.*[5].

Our three land-use classes are comprised of ample proportions of active land use, ranging from 75% for *cleared/cultivated* lands to 58% for *mosaic vegetation* (**Supplemental Figure 4a**). Active land use is correspondingly concentrated within these three land-use classes, as illustrated by these classes' positive deviations from the diagonal line in **Supplemental Figure 4b**. Such observations are consistent with the class descriptions and corresponding nominal land-management intensities described in **Table 1**. Notably, **Supplemental Figure 4b** also shows that *flooded vegetation* and *forest* comprise just over one-quarter of active land use. Within the realm of active land use, the proximity of these nominally unmanaged land covers to *mosaic cropland* underscores how declining fire-activity severity and ignitions over *mosaic cropland* (**Table 2**) may foment similar declines over *forest (***Table 2a***)*.

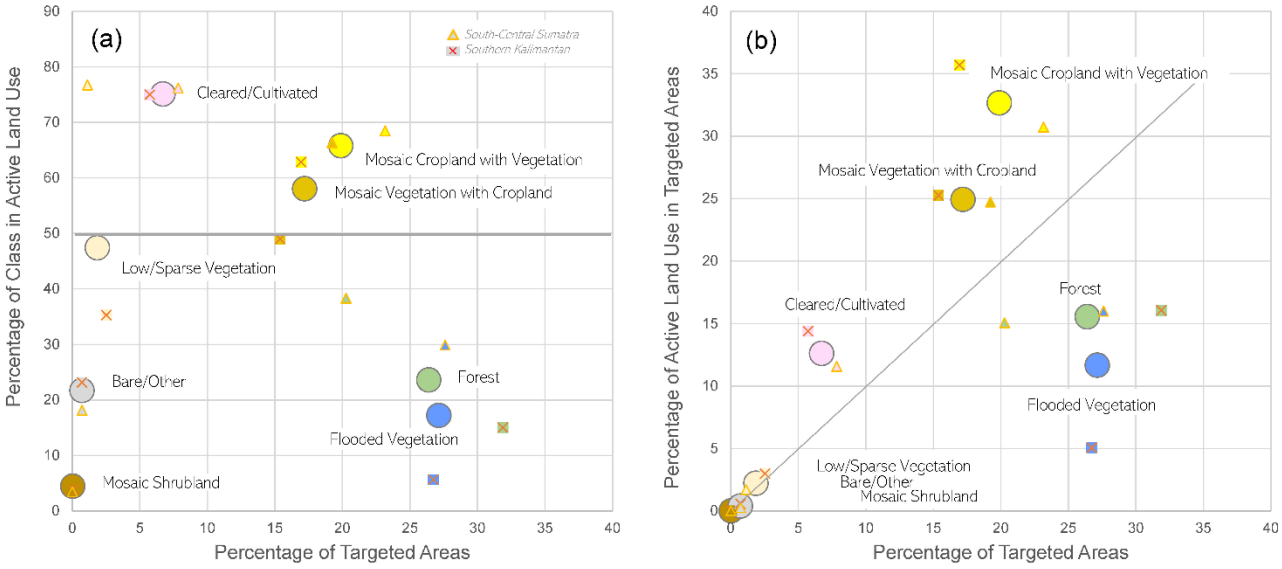

Supplemental Figure 4 (a) Percentage area of a land-use/cover class that is dedicated to active land use, and (b) Percentage of total active land-use area by land-use/cover class, for the Targeted Areas within the Fire-Affected Regions, 2015.

*****

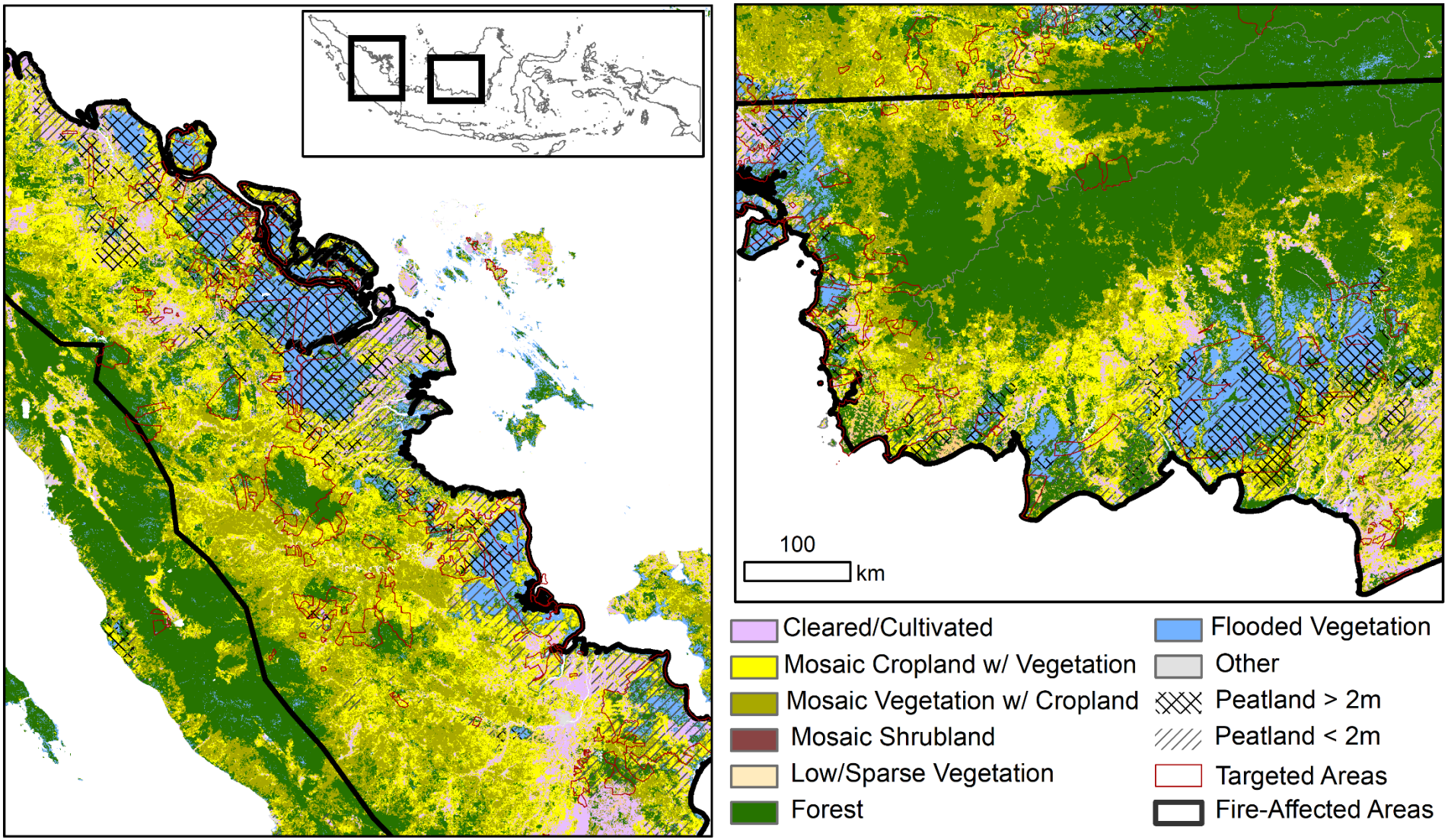

Supplemental Figure 5 Land-use/cover classes relative to Peatland and Targeted Areas, for Central-South Sumatra and Southern Kalimantan, 2015.

Original Class ID	Original Class	Aggregated Class	Percentage of AFDs in Original Class, Indonesia (2018)
10	Cropland, rainfed	Cleared/Cultivated	4
11	*Herbaceous cover*	Cleared/Cultivated	5.4
12	*Tree or shrub cover*	Cleared/Cultivated	5.7
20	Cropland, irrigated or post-flooding	Cleared/Cultivated	0.2
30	Mosaic cropland (>50%) / natural vegetation (tree, shrub, herbaceous cover) (<50%)	Mosaic Cropland	20.1
40	Mosaic natural vegetation (tree, shrub, herbaceous cover) (>50%) / cropland (<50%)	Mosaic Vegetation	21.5
50	Tree cover, broadleaved, evergreen, closed to open (>15%)	Forest	24.4
60	Tree cover, broadleaved, deciduous, closed to open (>15%)	Forest	
61	*Tree cover, broadleaved, deciduous, closed (>40%)*	Forest	
62	*Tree cover, broadleaved, deciduous, open (15-40%)*	Forest	
70	Tree cover, needleleaved, evergreen, closed to open (>15%)	Forest	
71	*Tree cover, needleleaved, evergreen, closed (>40%)*	Forest	
72	*Tree cover, needleleaved, evergreen, open (15-40%)*	Forest	
80	Tree cover, needleleaved, deciduous, closed to open (>15%)	Forest	
81	*Tree cover, needleleaved, deciduous, closed (>40%)*	Forest	
82	*Tree cover, needleleaved, deciduous, open (15-40%)*	Forest	
90	Tree cover, mixed leaf type (broadleaved and needleleaved)	Forest	
100	Mosaic tree and shrub (>50%) / herbaceous cover (<50%)	Mosaic Shrubland	0.8
110	Mosaic herbaceous cover (>50%) / tree and shrub (<50%)	Mosaic Shrubland	2.8
120	Shrubland	Low/Sparse Vegetation	0.2
121	*Evergreen shrubland*	Low/Sparse Vegetation	
122	*Deciduous shrubland*	Low/Sparse Vegetation	
130	Grassland	Low/Sparse Vegetation	<0.1
140	Lichens and mosses	Low/Sparse Vegetation	
150	Sparse vegetation (tree, shrub, herbaceous cover) (<15%)	Low/Sparse Vegetation	6.4
151	*Sparse tree (<15%)*	Low/Sparse Vegetation	
152	*Sparse shrub (<15%)*	Low/Sparse Vegetation	
153	*Sparse herbaceous cover (<15%)*	Low/Sparse Vegetation	
160	Tree cover, flooded, fresh or brackish water	Flooded Vegetation	4.4
170	Tree cover, flooded, saline water	Flooded Vegetation	0.5
180	Shrub or herbaceous cover, flooded, fresh/saline/brackish water	Flooded Vegetation	
190	Urban/Settled areas	Other	2.7
200	Bare areas	Other	
201	*Consolidated bare areas*	Other	
202	*Unconsolidated bare areas*	Other	
210	Water bodies	Other	0.1

Supplemental Table 6 Original Copernicus land-use/cover classes and corresponding aggregated classes of this study, alongside percentages of 2018 active-fire detections amongst the original classes as of 2018.

Notes: Percentages do not sum to 100 due to rounding. Percentages were calculated using land-use/cover data and MODIS AFD data as of 2018.

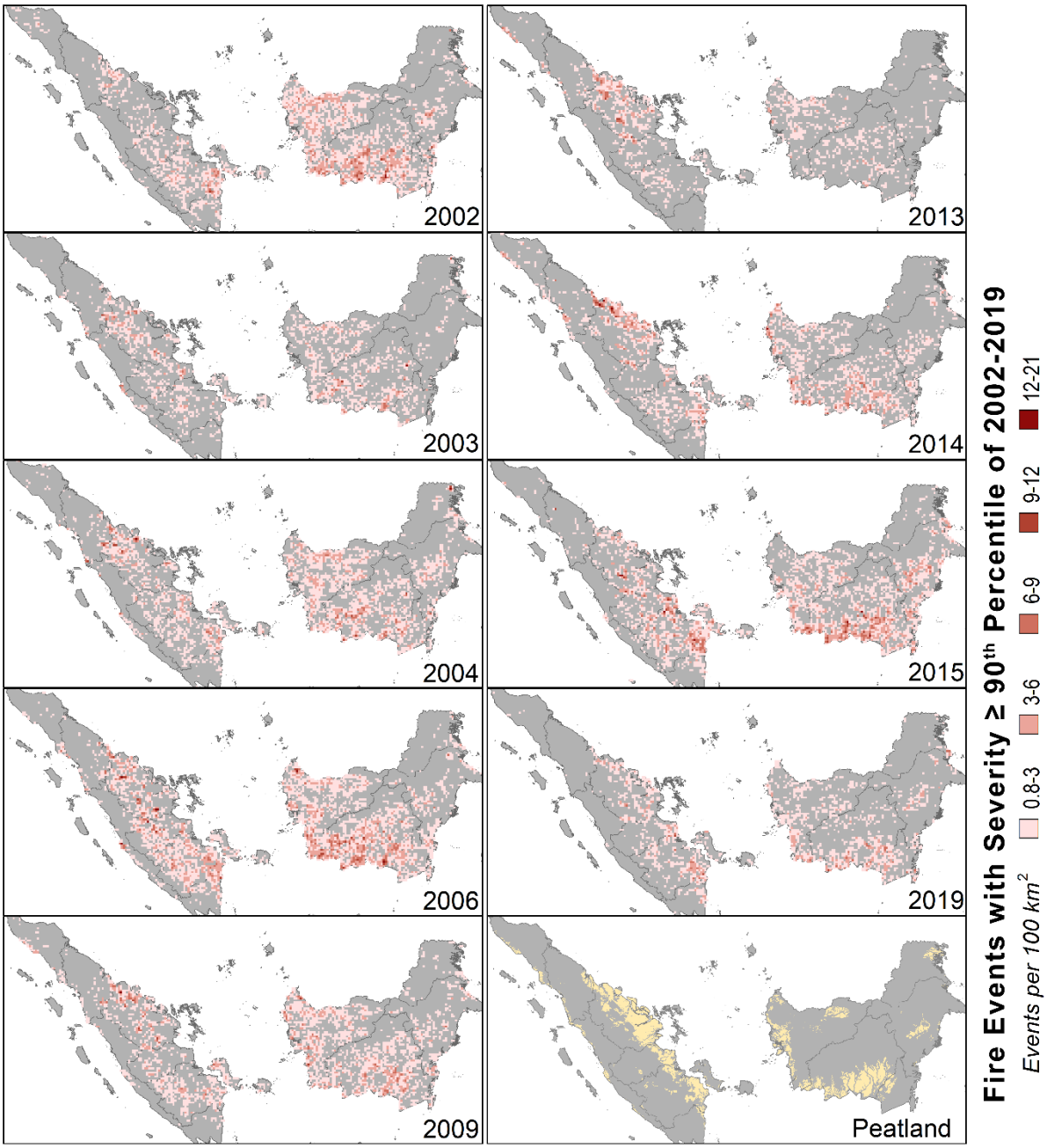

Supplemental Figure 6 Very severe fire events and Peatland in Sumatra and Kalimantan, Indonesia, for years of severe fire activity.

Notes: Years of severe fire activity are those for which ≥25% of fire events are severe.

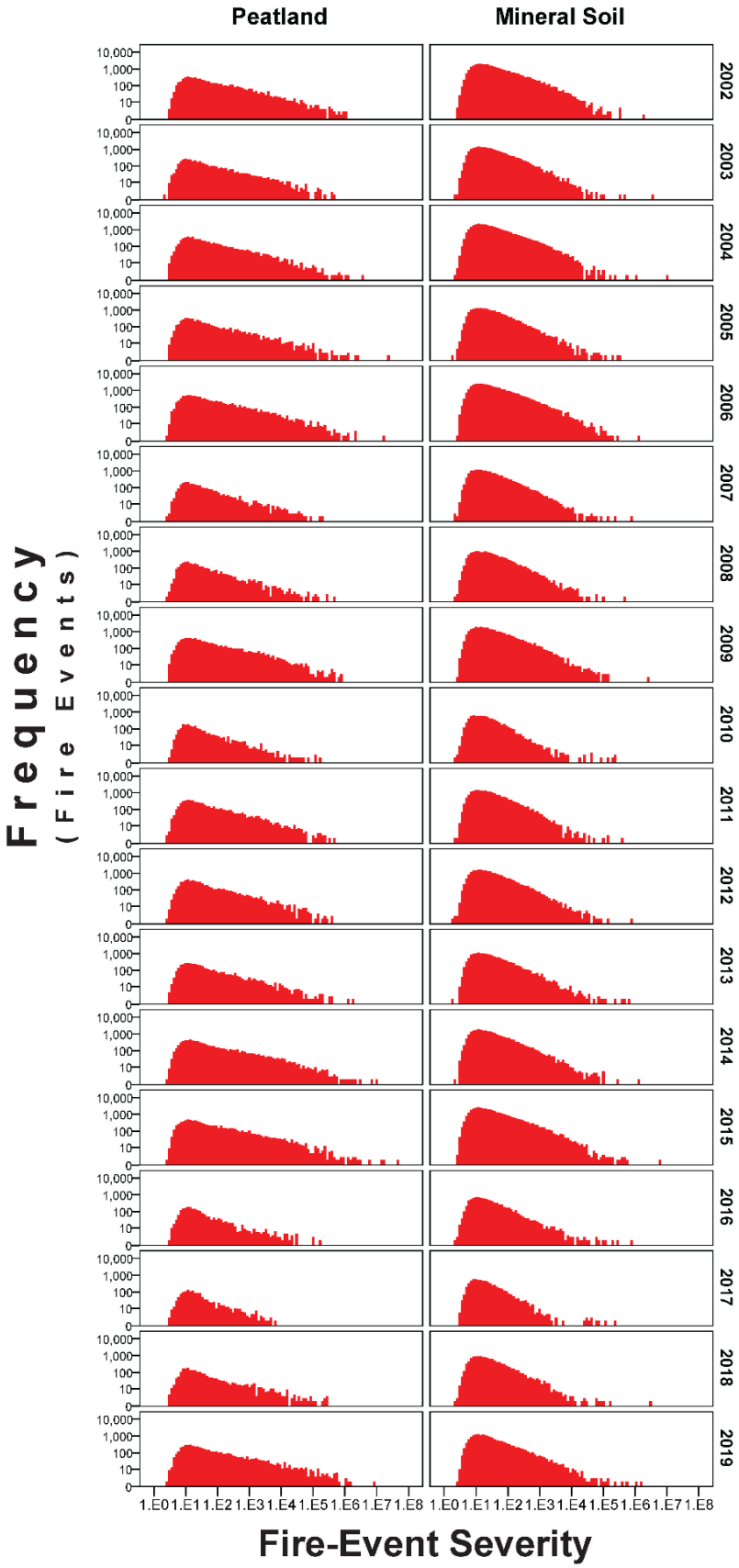

Supplemental Figure 7 Frequency of fire-event severity scores by year, for Peatland and mineral soils, 2002-2019, Indonesia.

	Percent of Fire-Event Scale Explained by Total Fire Radiative Power	
	Severe Fire Events	*Very Severe Fire Events*
Peatland	51	52
Mineral Soil	33	30

Supplemental Table 7 Percentage of fire-event scale explained by total fire radiative power, controlling for the number of active-fire detections per fire event.

Note: Values are squared partial correlation coefficients significant at $p<0.01$. Fire events were weighted by their respective severity scores (Eqn. 1) to account for the relative importance of individual events. Fire-event scale is defined by Eqn. 1. Total FRP, AFD frequency, and severity per fire event were logarithmically transformed to enhance linear fit.

Supplemental Note 4: Fire Events and Burned Areas

Fire events are spatio-temporal clusters of MODIS MCD14ML active-fire detections (AFDs) (**Figure 4**). Individual AFDs represent thermal anomalies indicative of one or more active fires in a given ~1 km^2 MODIS pixel[10]. AFD data do not indicate burned area (BA) at local scales, though AFD frequency and BA are highly correlated regionally[11-13]. Accordingly, fire events are best understood as discrete instances of fire activity integrated by local human agency and land-use systems and for which burning is often physically contiguous but not necessarily always so. Here, to qualify our fire events in terms of their degree of burning, we compared fire events to a variety of satellite-derived BA products below. For the purposes of aerial comparisons, we buffered fire-event AFDs by 500 meters (**Figure 4**), being roughly half the width of a MODIS pixel.

To summarise our results of the comparisons below, 24-46% of total fire-event buffer area was burned on average according to a Sentinel-2 BA estimate of 2019[14] for the fire-affected regions of Southern Kalimantan and Central-South Sumatra, with this proportion increasingly log-linearly with increasing fire-event severity. Comparisons of fire-event buffer areas against Landsat BA estimates in Central Kalimantan province and Central-South Sumatra for shorter periods over various years observed a similar estimate of 22-45% of buffer area burned. Note that BA estimates here are conservatively low, given the arbitrarily shape of our fire-event buffers and the greater tendency for BA data to overlook smaller, ephemeral, or cooler fires compared to our AFD data[12,14]. The following details each comparison of our fire-event buffer areas against BA estimates in turn.

4.1 Comparisons Against Sentinel-2 Burned Area Data in the Fire-Affected Regions

Fire events of 2019 were compared against the national 2019 BA product of Gaveau *et al.*[14] for Southern Kalimantan and Central-South Sumatra. This BA product is a classification of temporally-dense stacks of Sentinel-2 satellite imagery trained by visual interpretations of burned/unburned areas as well as by sudden spectral changes to land cover indicative of burning. User's and producer's accuracies are high compared to similar BA classifications, at 97-99% and 63-83%, respectively, according to validation against visually interpreted burn scars[14]. Given the annual temporal resolution of this 2019 BA classification, overlapping fire events and BA patches of 2019 were assumed to capture the same fire activity over a common period.

Nationally, 72% of AFDs in 2019 occurred within BAs of the Sentinel-2 classification. For fire events buffered by 500 m, BA as a percentage of fire-event buffer area varied between 24% and 46% on average (**Supplemental Table 8**). The lower estimate reflects the fact that the buffers of some, generally smaller/lower-severity fire events did not encompass any BA according to the Sentinel-2 classification (**Supplemental Figure 8**). Such events are presumed to be instances of BA omission error, not AFD commission error, as BA omission error is generally high[12,14] compared to MODIS AFD commission

error[10,11,13,15]. To account for BA omission error, we excluded fire events without any corresponding BA and re-estimated the mean percentage buffer area that burned, at 40% (**Supplemental Table 8**).

Notably, as fire-event severity increased, the percentage of all fire-event buffers comprised by BA also steadily increased while the variability thereof decreased (**Supplemental Figure 8**). This relationship affirms the fidelity of our fire-event severity measure (Eqn. 1) and is consistent with correlations between regional AFD frequency and BA[11-13]. In light of this relationship, we re-estimated the percentage fire-event buffer area that burned after weighting fire events by their respective ADF frequencies. The weighted means percentages of buffer areas that burned were slightly to moderately greater than the unweighted means, at 39 to 46% (**Supplemental Table 8**).

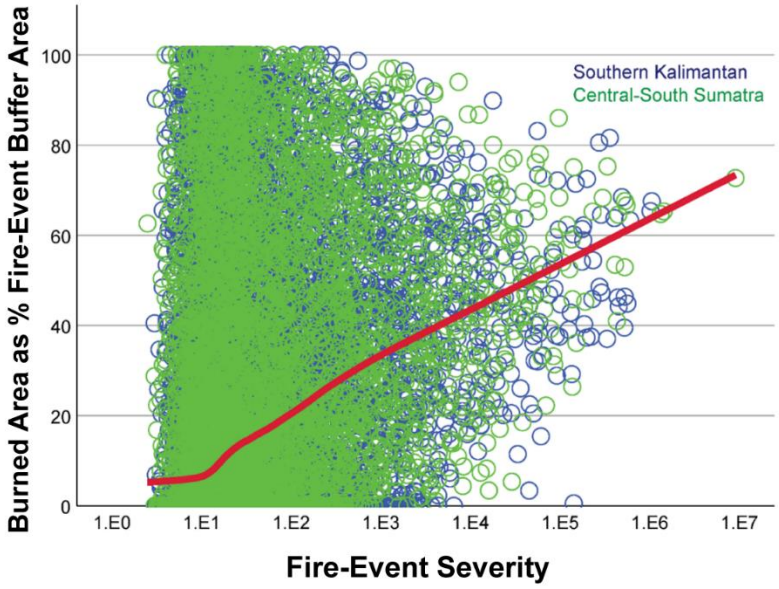

Supplemental Figure 8 Burned area as a percentage of 500-m buffer areas surrounding fire events, Southern Kalimantan and Central-South Sumatra, 2019.

Notes: Burned area as of 2019 is as defined by Sentinel-2 satellite estimates by Gaveau *et al.*[14]. Fire events are as specified for this study, here for 2019, buffered by 500-m in order to observe their spatial overlap with burned areas. The trend line is defined by an iteratively-weighted lest-squares Epanechnikov loess function robust to outliers[16]. The trend line includes fire events without corresponding burned areas. Note the logarithmic scale of the x-axis.

Set of Fire Events	Fire-Event Buffer that is Burned (Mean %)	Fire-Event Buffer that is Burned (Mean %), Weighting by Event AFD Frequency
Including Events with no Burned Area	24	39
Excluding Events with no Burned Area	40	46

Supplemental Table 8 Percentage area of fire-event buffers that are burned according to Sentinel-2 burned-area estimates, for Southern Kalimantan and Central-South Sumatra, 2019.

4.2 Comparisons against Landsat Burned Area Data in Central Kalimantan

We also compared our fire events of 2003-2015 against Landsat-classified BAs for the Mawas area of Central Kalimantan province – a 53,000 ha tract of degraded peatlands prone to burning (2°21'20.03" S 114°32'01.72" E). Landsat TM/ETM/OLI classifications of BA produced by the NASA Carbon Monitoring System[17] were trained using visually-interpreted burned/unburned sites, with MODIS MCD14ML AFD data helping distinguish pre-fire from post-fire conditions. Classification accuracies are reportedly ~98%[17], though no validation methods or omission-error data were reported. Given the annual temporal resolution of the Landsat classifications, comparisons between the BAs and our fires events again presume that spatial overlap between the data is due to each dataset capturing local burning over a common period of a given year.

Supplemental Table 9 summarises the comparison for the Mawas area. A median and mean of 41% and 45% of fire-event buffer area was classified as burned between 2003 and 2015 in the Mawas area, respectively. BAs outside fire events were less extensive but still appreciable, equivalent to 17% (mean) or 21% (median) of fire-event buffer area in the Mawas area. Estimated percentages of buffer areas that burned in the Mawas area may be higher than typical for Indonesia, given the extensiveness of burning in the Mawas area, but are consistent with upper estimates based on the Sentinel-2 BA product (**Supplemental Table 8**). On the other hand, the estimated percentages of buffer areas that burned may be relatively depressed, and omission rates inflated correspondingly (right column of **Supplemental Table 9**), given that AFD data tend to have elevated omission rates for low-temperature smouldering peatland fires where such fires are not hot or large[18,19].

Year	Burned Area Inside Fire-Event Buffer, as a Percent of Buffer Area	Burned Area Outside Fire-Event Buffers, as a Percent of Buffer Area
2003	19	20
2004	40	12
2005	53	9
2006	64	15
2007	4	40
2009	58	10
2011	31	26
2012	41	12
2013	41	17
2014	64	49
2015	83	25
Median	41	17
Mean	45	21

Supplemental Table 9 Burned area within fire-event buffer areas, according to Landsat classifications in the Mawas peatlands of Central Kalimantan, 2003-2015.

Note: No Landsat classifications were produced for 2008 and 2010.

4.3 Comparisons against Landsat Normalised Burned Ratio Data in Kalimantan and Sumatra

We further compared fire events against Landsat-estimated BAs across a diversity of landscapes and years in Sumatra and Kalimantan. We defined a burned/unburned reference layer by calculating change to the Normalised Burned Ratio metric between pairs of Landsat images. Given two Landsat Normalised Burned Ratio (NBR) images acquired within 90 days of each another, any area for which NBR values increased by >0.15 was classified as burned. This ΔNBR threshold reflects ground knowledge and visual inspections of burn scars in Landsat imagery, and was also adopted by Cattau *et al.*[20] and Sloan *et al.*[5] for similar qualifications of Indonesian fire events. All Landsat imagery had ≤10% cloud cover and was radiometrically and geometrically corrected to Precision Terrain Tier 1 standards. Areas with cloud cover, cloud shadow, or open water were excluded to prevent spurious ΔNBR values.

We focused on parts of Central-South Sumatra (Riau, South Sumatra, and Jambi provinces) and Central Kalimantan province hosting major conglomerations of Targeted Areas (**Supplemental Figure 1**). Comparisons also included extensive areas adjacent to these Targeted Areas that were encompassed by the Landsat images. For Sumatra, a search for Landsat TM, ETM, and OLI images acquired between 2001 to 2019 identified three image pairs for three Landsat scenes (**Supplemental Table 10**). For Kalimantan, a search for the scenes previously surveyed by Cattau *et al.*[20] yielded two image pairs for a single scene (**Supplemental Table 10**). Landsat ETM imagery of May 2003-2019 was not considered due to its SLC-off data error. Comparisons considered all fire events for which ignitions occurred during the period spanned by a given Landsat ΔNBR image pair.

Results of the comparisons are summarised in (**Supplemental Table 10**). The percentage of fire-event buffer area classified as burned ranged from 6% to 45% across all five Landsat scenes. Higher measures for a given scene correspond to relatively extensive fire activity and early-to-mid fire seasons coincident with El Niño periods, when fire activity is historically elevated. Upon weighting scenes by their respective areas of fire-event buffers, an overall average of 35% of buffer area is observed as burned. The tendency towards greater proportions of fire-event buffers in BAs given greater total fire activity, as well as the range of estimates in question, are consistent with the comparisons of fire events against the Sentinel-2 BA product above.

	Period of ΔNBR Image Pair	Burned Area Inside Fire-Event Buffer, as a Percent of Buffer Area	Landsat Scene Location (WRS2 Path / Row)	Landsat Sensor (TM, ETM, OLI)	Fire-Event Buffer Area (km^2)
Central-South Sumatra	*30 June - 17 August, 2002*	26	124/62	ETM	450.0
	5 July - 6 August, 2016	6	125/62	OLI	34.9
	26 June - 12 July, 2016	7	126/60	OLI	58.3
Sumatra Average*		**22**			
Central Kalimantan	16 May - 17 June, 2004	9	118/62	TM	13.4
	20 August - 21 September, 2004	45	118/62	TM	685.8
Kalimantan Average*		**44**			
Overall Average*		**35**			

Supplemental Table 10 Burned area within fire events according to Landsat ΔNBR data.

Notes: (*) Overall and per-island averages are weighted by the fire-event buffer areas of respective Landsat scenes.

*****

Supplemental Note 5: Fire-Event Severity Scores from Active-Fire Detection vs. Burned-Area Data

5.1 Fire-Event Severity Distributions for AFD and BA Fire Events

For comparison against our measures of fire-event severity (Eqn. 1) based on MODIS MCD14ML active-fire detections (AFDs), we defined an analogous fire-event severity index for Indonesian fire events of the Global Fire Atlas described by Andela *et al.*[21,22] between January 2003 and November 2018 using MODIS MCD64a1 500-m burned area (BA) data[23]:

$$\text{Fire-Event Severity}_{BAi} = \text{Fire Event Area} \times \text{Fire Event Duration} \quad \text{(S2)}$$

where, for the i^{th} fire event, *Area* is the extent of the fire event in square kilometres, and *Duration* is as for Eqn. 1 but estimated *post facto* according to the spectral signatures of burned pixels[23]. Eqn. S2 describes fire-event scale in terms of *Area, not* $\sum FRP$ as in Eqn. 1, because BA data do not observe FRP while AFD data are unsuited to estimate BA locally. First-order comparisons may be cautiously entertained between the general shapes of fire-event severity frequency distributions from Eqn. 1 and Eqn. S2 (**Supplemental Figure 1**), while differences between MODIS AFD and BA data preclude direct comparisons. Units are not comparable between the two indices.

Frequency distributions of our measure of fire-event severity (Eqn. 1) are significantly more skewed than distributions of analogous severity scores for fire events of the Global Fire Atlas (Eqn. S2; $p<0.001$, Kolmogorov-Smirnov test of equivalent histogram shape based on index percentiles, 2003-2018). Distributions of our measure of fire-event severity have much longer tails than distributions for the Global Fire Atlas (**Supplemental Figure 9, Supplemental Figure 10**), both for years of severe fire activity (≥25% of fire events are severe) and all other years, suggesting greater extremes amongst discrete fire events than previously indicated. Greater extremes amongst our fire events likely reflect (*i*) the tendency for relatively large, radiative, and/or persistent fires tend to have more AFDs for a given burned area[24,25], as well as greater fire radiative power per AFD[26], so boosting the scale and thus severity of our fire events; and (*ii*) the fact that AFD data capture more fire activity across mosaic agricultural lands and tropical forests[24,27] common in Indonesia, as well as ephemeral fire activity, possibly integrating larger fire events.

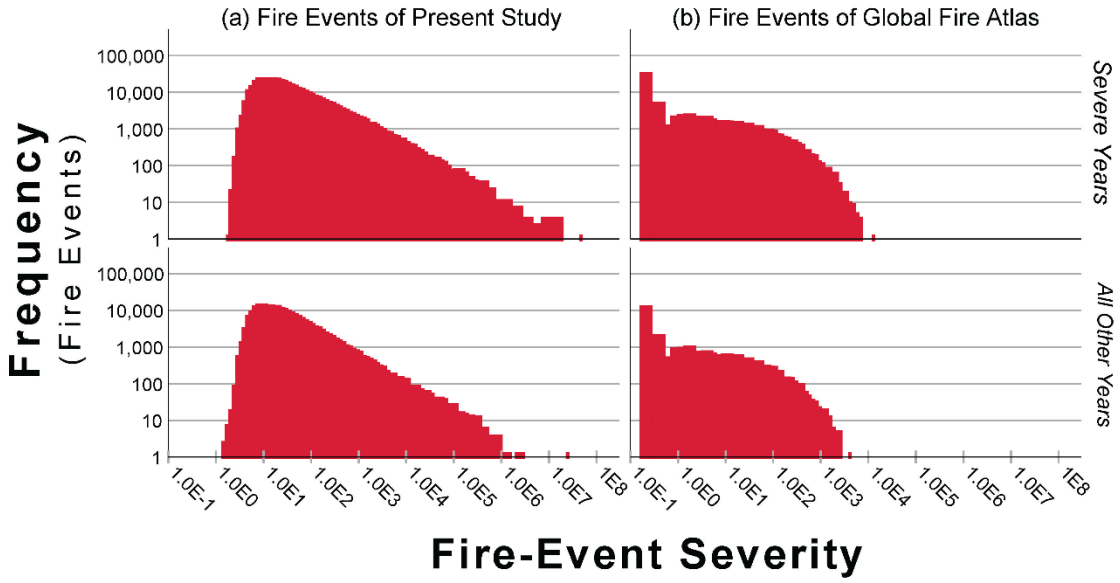

Supplemental Figure 9 Frequency of fire-event severity scores for fire events defined by (a) Active-fire data of this study and (b) Burned-area data of the Global Fire Atlas.

Notes: Years severe fire activity ('severe years') are 2002, 2003, 2004, 2006, 2009, 2013, 2014, 2015 and 2019. Fire events of the Global Fire Atlas are as defined by Andela *et al.*[21,22]. Fire-event severity scores for (*a*) and (*b*) are given by Eqn. 1 and Eqn. S2, respectively. Scores are not comparable between (*a*) and (*b*). Note the logarithmic scales.

The measures of fire-event severity defined for our study (Eqn. 1) and for the fire events of the Global Forest Atlas (Eqn. S2) are analogous in that both describe severity according to interactions between fire-event scale and duration. Direct comparisons are however precluded by inherent differences between underlying AFD and BA data. These differences respectively pertain to (*a*) spatial structure (points vs. pixels), (*b*) fire-detection methods (local thermal anomalies vs. burned-cover spectral signatures), (*c*) sensitivity to fire activity (higher vs. lower), (*d*) temporal accuracy (direct daily observation vs. post-facto estimation of day of burning), and (*e*) fire-activity recording rate[10,23,27,28]. The latter difference refers to the fact that, for a given geographic coordinate, AFDs of ~1-km spatial resolution may be recorded repeatedly over successive days of fire activity, while a BA pixel of ~500-m resolution may be recorded as burned only once over successive days. This possibility warrants caution when comparing the skewness of the fire-event severity frequency distributions defined by AFD data and BA data in **Supplemental Figure 1**. Specifically, for each additional day of fire-event duration, if the scale of an AFD-based fire event (∑FRP in Eqn.1) should increase more rapidly than the scale of a BA-based fire event (km^2 in Eqn. S2), then skewness (Eqn. 2) may be greater for the AFD-derived fire events than the BA-derived fire events in **Supplemental Figure 1** without necessarily capturing greater extremes of fire activity. There is however no clear evidence of such a trend for our context generally, notwithstanding the partial exception of point (*i*) below pertaining to certain larger fire events. In fact, regression analyses of standardised scores of fire-event scale on duration indicate that, for our AFD-derived events, the rate of

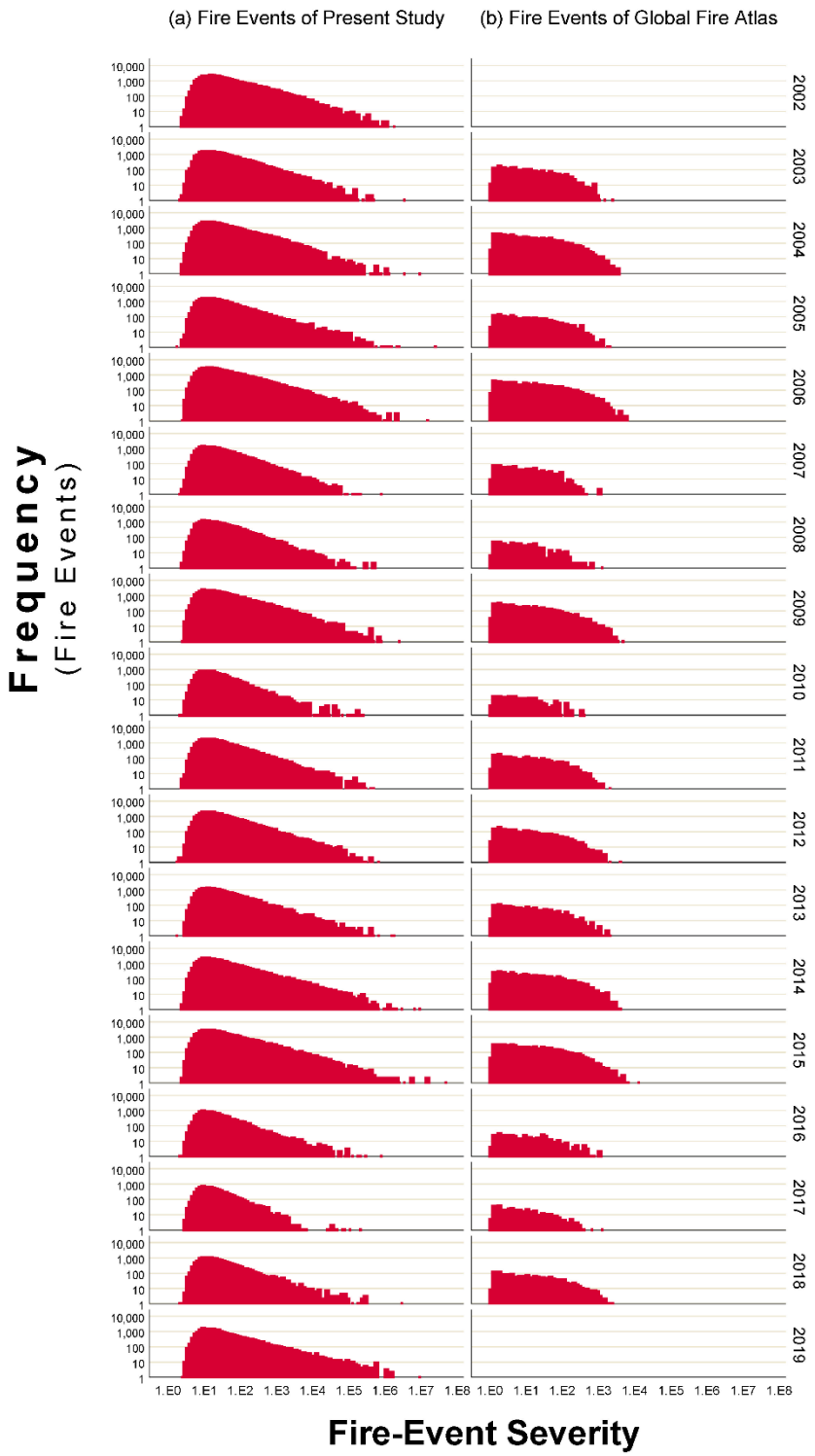

Supplemental Figure 10 Frequency of fire-event severity scores by year, for fire events defined by (a) Active-fire detection data of this study and (b) Burned-area data of the Global Fire Atlas, Indonesia.

Notes: Fire events of the Global Fire Atlas are as defined by Andela *et al.*[21,22]. Fire-event severity scores for columns (*a*) and (*b*) are given by Eqn. 1 and Eqn. S2, respectively. Values are not comparable between (*a*) and (*b*). Note the logarithmic scales. No data exists for 2002 and 2019 for (*b*).

increase to scale given increase to duration is less than half that for BA-derived events on average. This discrepancy in rates reflects the weaker linear relationship between scale and duration for AFD-derived fire events ($r=0.27$, $p<0.01$) compared to BA-derived fire events ($r=0.64$, $p<0.01$).

5.2 Advantages of Fire-Event Severity as Described by AFD Data

With respect to describing fire-event severity, the MODIS MCD14ML AFD data we use have certain advantages over the MODIS MCD64A1 BA data used by Andela *et al.*[21] to define fire events for the Global Fire Atlas. Our AFD data capture more fire activity across croplands and tropical forests[24,27], especially where fires are ephemeral or smaller, and so are well suited to the Indonesian context. Also, the BA data tend to omit dispersed, smaller-scale, and/or ephemeral fire activity[12,14] (e.g., agricultural fires or interstitial burning between larger fire fronts), a fact which may depress measures of fire-event scale and duration for BA-derived fire events in Eqn. S2, consistent with **Supplemental Figure 1**. Given such omissions, we refrained from spatio-temporally integrating our AFD-derived fire events with the BA-derived fire events of Andela *et al.*[21],

as to observe fire-event severity in terms of event area, duration, and fire radiative power (FRP). Indeed, previous attempts at such integration report large proportions of 'unpaired' fire events between the AFD and BA data[5,29].

Fire-activity extremes are well profiled against the relatively extensive and diverse burning captured by AFD-derived fire events. The following AFD data attributes illustrate their utility to this end:

(i) Extensive, persistent, intense fire activity tends to yield more AFDs for a given nominal burned area[24,25,29]. The dense cluster of AFDs comprising Fire Event 2 in **Supplemental Figure 11b** is illustrative of this attribute. Our measure of fire-event severity, which incorporates AFD frequency (Eqn. 1), would therefore reflect the scale of large, intensive, and/or persistent fire events more comprehensively than would the severity index for BA data (Eqn. S2).

(ii) Our AFD data allow for fire-event scale to be estimated as a function of total FRP per event (Eqn. 1). Total FRP covaries with AFD frequency per event but also correlates with the biomass consumption rate of a given event[30]. FRP thus expands the scope of our fire-event severity index from event magnitude to event intensity, as demonstrated by Peatland-vs-mineral soil comparisons in **Supplemental Table 7**. Greater sensitivity to ephemeral or small-scale burning means that lower-intensity fringes of larger fire events may be captured more fully[11] by the AFD data, again increasing fire-event scale and thus severity, including by inter-connecting nodes of burning into larger fire events. Indeed, the greater extremes of our fire-event data compared to the fire events of the Global Fire Atlas (**Supplemental Figure 9**) may reflect the priority given by Andela *et al.*[21] to splitting contiguous BAs into discrete fire events according post-facto estimations of fire chronology (Fire Event 1 in **Supplemental Figure 11b**).

(iii) Our time series is longer than that the BA-derived fire events of the Global Fire Atlas[21,22], which presently omits 2002 and 2019, each host to El Niño periods during which both fire activity and drought were severe (**Supplemental Figure 6, Figure 1c**).

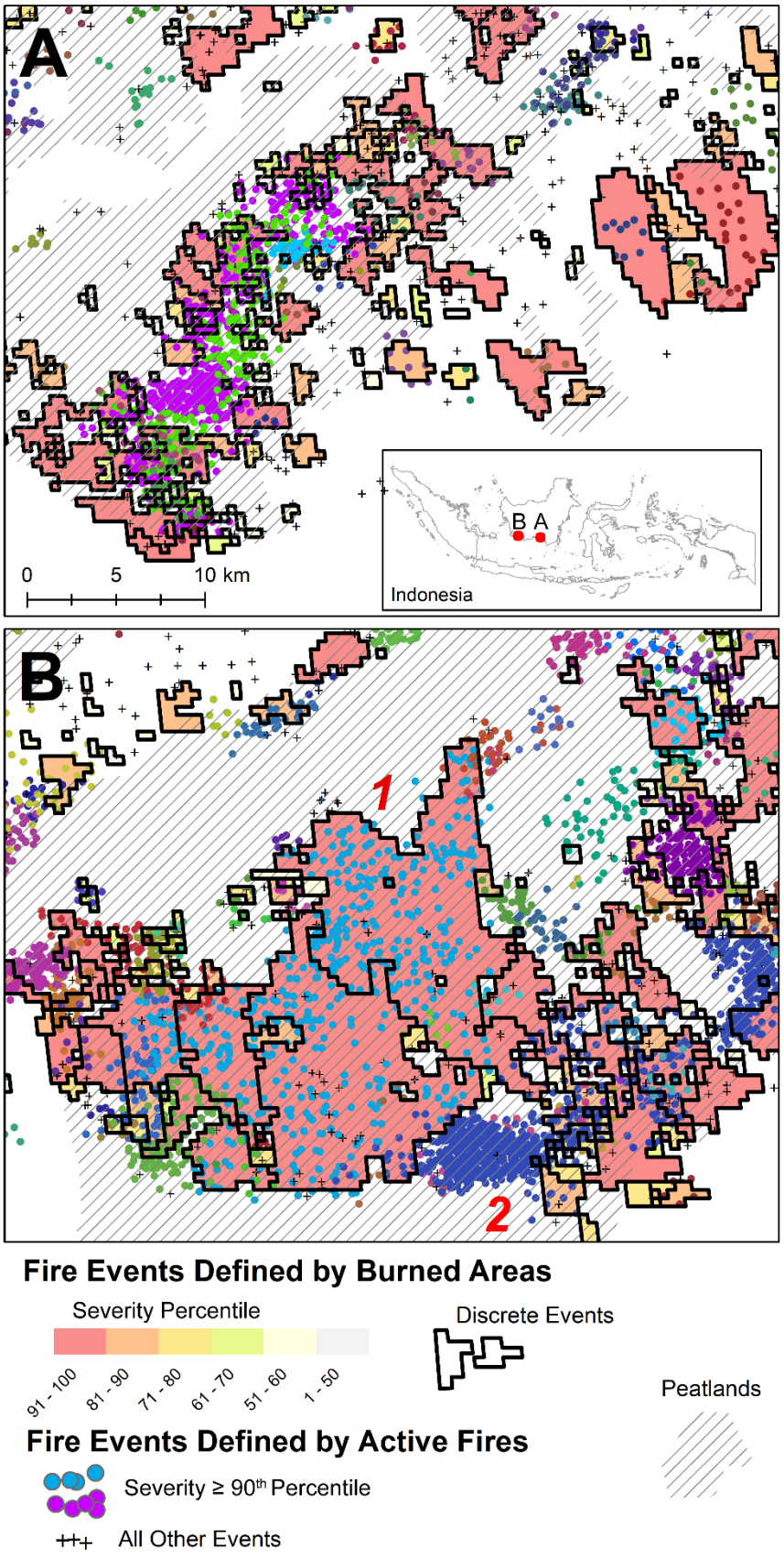

Supplemental Figure 11 Fire events derived from MODIS active-fire detection data and MODIS burned-area data, with corresponding fire-event severity scores, for two areas of peatland in Southern Kalimantan, 2015.

Notes: The locations of panels A and B are shown in the inset map. All fire events are for 2015. Fire events defined by burned-area data are as per the Global Fire Atlas and described by Andela *et al.*[21,22]. Percentiles for fire-event severity are with respect to all fire events nationally over 2002-2019 (active-fire detections) or 2003-2018 (burned areas).For fire events derived from active-fire detections, only those events with severity scores >90th percentile are shown as discrete. All other events of 2015 are visible but not shown as discrete. Red numbers labelled as 1 and 2 in panel B identify two notable fire events defined by active-fire detections, discussed in Supplemental Note 5.

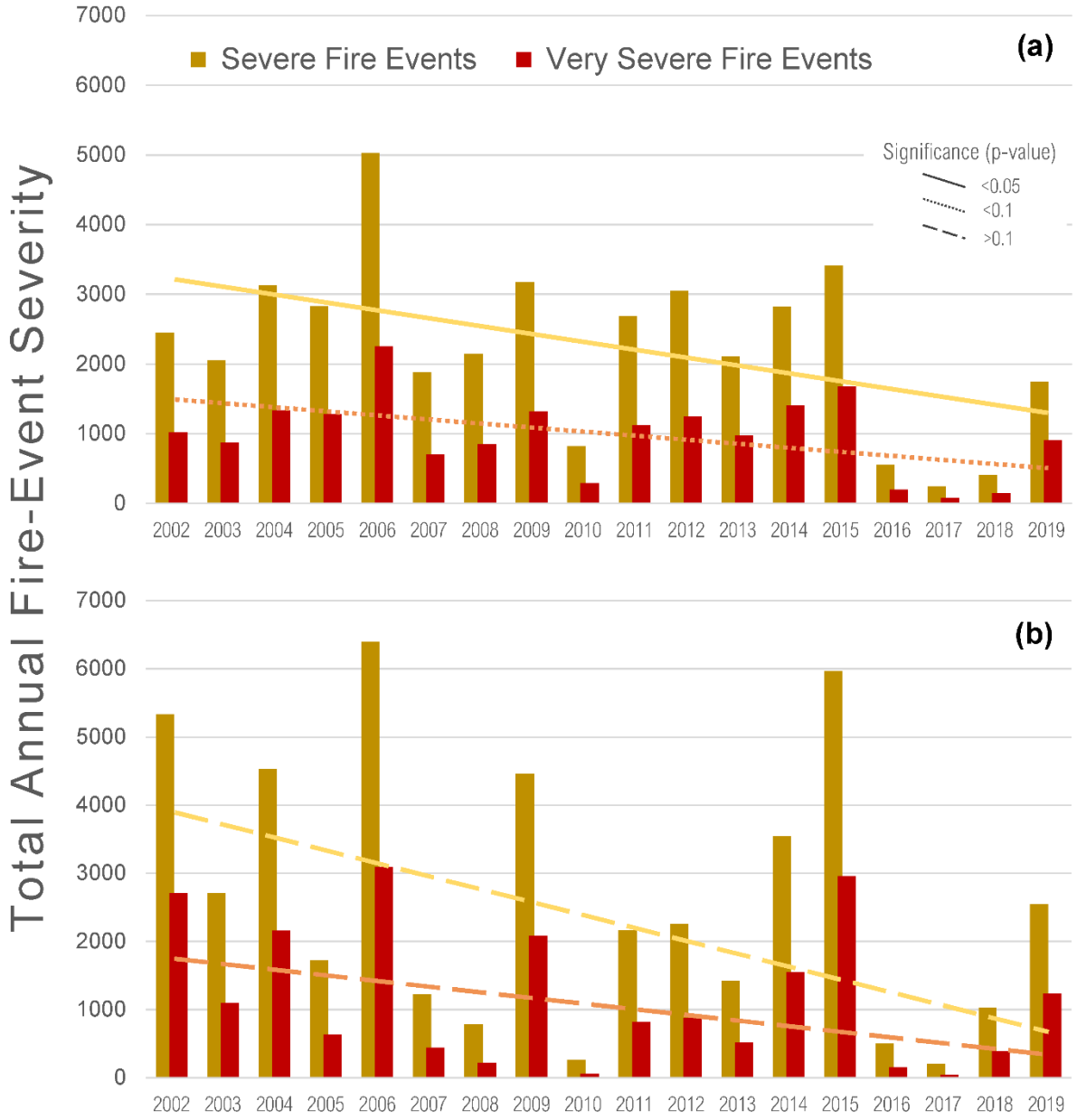

Supplemental Figure 12 Trends in the total annual fire-event severity of severe or very severe fire events in (a) Central-South Sumatra and (b) Southern Kalimantan over 2002-2019.

Notes: >95% of the total fire-event severity of all fire events is accounted for by severe fire events alone. Graphed linear trends are as per regressions of total annual fire-event severity on time elapsed since 2002, without controlling for precipitation. Regressions were bootstrapped and unweighted. Weighting the regressions with respect to annual AFD frequencies defined negative, but statistically insignificant, trends.

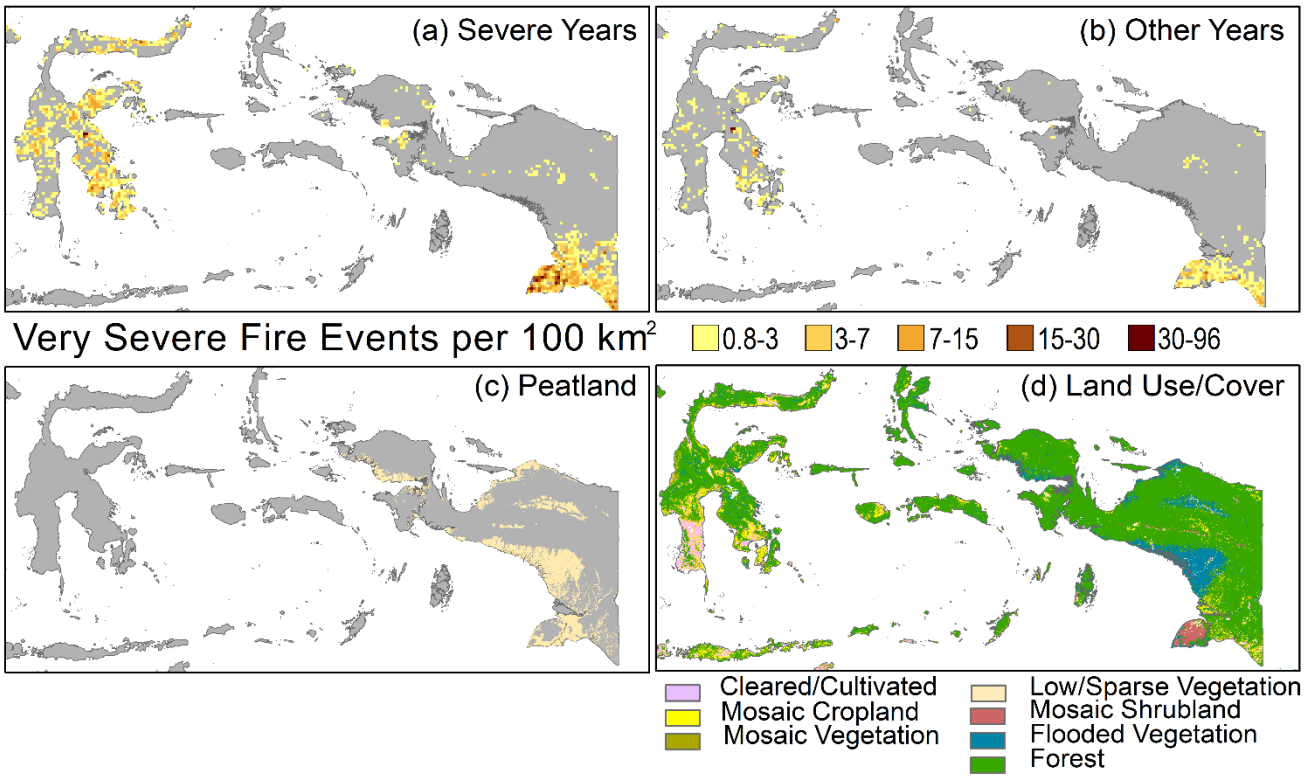

Supplemental Figure 13 Density of very severe fire events in Sulawesi and Papua, Indonesia for (a) years of severe fire activity during 2002-2019 and (b) all other years, relative to (c) Peatland and (d) land-use/cover classes as of 2015.

Notes: Years severe fire activity in (*a*) are those for which ≥25% of fire events are severe, i.e., 2002, 2003, 2004, 2006, 2009, 2013, 2014, 2015 and 2019. In (*d*), classes are adapted from the Copernicus Climate Change Initiative Land-Cover Product[31,32] (**Table 1**). **Figure 2** repeats panels (a) through (d) for other areas of Indonesia.

Supplemental References

1 Mahmoudi, M. R., Nasirzadeh, R., Baleanu, D. & Pho, K.-H. The properties of a decile-based statistic to measure symmetry and asymmetry. *Symmetry* **12,** 296, (2020).

2 Joanes, D. N. & Gill, C. A. Comparing measures of sample skewness and kurtosis. *Journal of the Royal Statistical Society. Series D (The Statistician)* **47,** 183-89, (1998).

3 Bono, R., Arnau, J., Alarcón, R. & Blanca, M. J. Bias, precision, and accuracy of skewness and kurtosis estimators for frequently used continuous distributions. *Symmetry* **12**, (2020).

4 Null, J. *El Niño and La Niña Years and Intensities Based on Oceanic Niño Index (ONI)*, Golden Gate Weather Services, http://ggweather.com/enso/oni.htm (2021).

5 Sloan, S., Tacconi, L. & Cattau, M. E. Fire prevention in managed landscapes: Recent successes and challenges in Indonesia. *Mitigation and Adaptation Strategies for Global Change* **26,** Article 32, (2021).

6 Savin, N. E. & White, K. J. The Durbin-Watson test for serial correlation with extreme sample sizes or many regressors. *Econometrica* **45,** 1989-96, (1977).

7 Fanin, T. & van der Werf, G. R. Precipitation–fire linkages in Indonesia (1997–2015). *Biogeosciences* **14,** 3995-4008, (2017).

8 Huijnen, V. *et al*. Fire carbon emissions over maritime Southeast Asia in 2015 largest since 1997. *Scientific Reports* **6,** 26886, (2016).

9 Armstrong, R. A. When to use the Bonferroni correction. *Ophthalmic and Physiological Optics* **34,** 502-08, (2014).

10 Giglio, L., Schroeder, W. & Justice, C. O. The Collection 6 MODIS active fire detection algorithm and fire products. *Remote Sensing of Environment* **178,** 31-41, (2016).

11 Tansey, K., Beston, J., Hoscilo, A., Page, S. E. & Paredes Hernández, C. U. Relationship between MODIS fire hot spot count and burned area in a degraded tropical peat swamp forest in Central Kalimantan, Indonesia. *Journal of Geophysicial Research* **113**, (2008).

12 Miettinen, J., Langner, A. & Siegert, F. Burnt area estimation for the year 2005 in Borneo using multi-resolution satellite imagery. *International Journal of Wildland Fire* **16**, (2007).

13 Hantson, S., Padilla, M., Corti, D. & Chuvieco, E. Strengths and weaknesses of MODIS hotspots to characterize global fire occurrence. *Remote Sensing of Environment* **131,** 152-59, (2013).

14 Gaveau, D. L. A., Descales, A., Salim, M. A., Shields, D. & Sloan, S. Refined burned-area mapping protocol using Sentinel-2 data increases estimate of 2019 Indonesian burning. *Earth System Science Data***,** https://doi.org/10.5194/essd-2021-113, (2021).

15 Tanpipat, V., Honda, K. & Nuchaiya, P. MODIS hotspot validation over Thailand. *Remote Sensing* **1,** 1043-54, (2009).

16 Jacoby, W. G. Loess: A non-parametric, graphical tool for depicting relationships between variables. *Electoral Studies* **19,** 577-613, (2000).

17 Vetrita, Y. & Cochrane, M. A. *Annual Burned Area from Landsat, Mawas, Central Kalimantan, Indonesia, 1997-2015*, ORNL Distributed Active Archive Center, www.doi.org/10.3334/ORNLDAAC/1708, https://daac.ornl.gov/CMS/guides/Annual_Burned_Area_Maps.html; https://daac.ornl.gov/cgi-bin/dataset_lister.pl?p=33 (2019).

18 Giglio, L., Descloitres, J., Justice, C. O. & Kaufman, Y. J. An enhanced contextual fire detection algorithm for MODIS. *Remote Sensing of Environment* **87,** 273-82, (2003).

19 Siegert, F. *et al.* Peat fires detected by the BIRD satellite. *International Journal of Remote Sensing* **25,** 3221-30, (2004).

20 Cattau, M. E. *et al.* Sources of anthropogenic fire ignitions on the peat-swamp landscape in Kalimantan, Indonesia. *Global Environmental Change* **39,** 205-19, (2016).

21 Andela, N. *et al.* The Global Fire Atlas of individual fire size, duration, speed, and direction. *Earth Systems Science Data* **11,** 529-52, (2019).

22 Andela, N., Morton, D. C., Giglio, L. & Randerson, J. T. *Global Fire Atlas with Characteristics of Individual Fires, 2003-2016*, ORNL Distributed Active Archive Center, www.doi.org/10.3334/ORNLDAAC/1642, https://daac.ornl.gov/cgi-bin/dsviewer.pl?ds_id=1642 (2019).

23 Giglio, L., Boschetti, L., Roy, D. P., Humber, M. L. & Justice, C. O. The Collection 6 MODIS burned area mapping algorithm and product. *Remote Sensing of Environment* **217,** 72-85, (2018).

24 Earl, N. & Simmonds, I. Spatial and temporal variability and trends in 2001–2016 global fire activity. *Journal of Geophysical Research: Atmospheres* **123,** 2524-36, (2018).

25 Miettinen, J., Shi, C. & Liew, S. C. Fire distribution in Peninsular Malaysia, Sumatra and Borneo in 2015 with special emphasis on peatland fires. *Environmental Management* **60,** 747-57, (2017).

26 Luo, R., Hui, D., Miao, N., Liang, C. & Wells, N. Global relationship of fire occurrence and fire intensity: A test of intermediate fire occurrence-intensity hypothesis. *Journal of Geophysical Research: Biogeosciences* **122,** 1123-36, (2017).

27 Roy, D. P., Boschetti, L., Justice, C. O. & Ju, J. The Collection 5 MODIS burned area product — Global evaluation by comparison with the MODIS active fire product. *Remote Sensing of Environment* **112,** 3690-707, (2008).

28 Justice, C. O. *et al.* The MODIS fire products. *Remote Sensing of Environment* **83,** 244-62, (2002).

29 Laurent, P., Mouillot, F., Moreno, M. V., Yue, C. & Ciais, P. Varying relationships between fire radiative power and fire size at a global scale. *Biogeosciences* **16,** 275-88, (2019).

30 Wooster, M. J., Roberts, G., Perry, G. L. W. & Kaufman, Y. J. Retrieval of biomass combustion rates and totals from fire radiative power observations: FRP derivation and calibration relationships between biomass consumption and fire radiative energy release. *Journal of Geophysical Research: Atmospheres* **110**, (2005).

31 Pérez-Hoyos, A., Rembold, F., Kerdiles, H. & Gallego, J. Comparison of global land cover datasets for cropland monitoring. *Remote Sensing* **9**, (2017).

32 ESA. *Annual land-cover product, 1992 to 2019/present, based on MERIS 300-m and ancillary SPOT, AVHRR, Sentinel-3 and PROB-V satellite data*. European Space Agency (ESA) European Centre for Medium-Range

Weather Forecasts (ECMFW) Copernicus Climate Change Service (C3S) Climate Change Initiative (CCI), https://cds.climate.copernicus.eu/cdsapp#!/dataset/satellite-land-cover?tab=overview; http://maps.elie.ucl.ac.be/CCI/viewer/download.php; http://www.esa-landcover-cci.org/ (2020).